Results in Physics 11 (2018) 315–324

Contents lists available at ScienceDirect

Results in Physics

journal homepage: www.elsevier.com/locate/rinp

Experiment and modeling of vibro-acoustic response of a stiffened submerged cylindrical shell with force and acoustic excitation

Xianzhong Wang[a,b,*], Di Chen[b], Yeping Xiong[c], Quanzhou Jiang[b], Yingying Zuo[b]

[a] Key Laboratory of High Performance Ship Technology (Wuhan University of Technology), Ministry of Education, Wuhan 430063, PR China
[b] Departments of Naval Architecture, Ocean and Structural Engineering, School of Transportation, Wuhan University of Technology, Wuhan 430063, PR China
[c] Faculty of Engineering and the Environment, University of Southampton, Southampton SO17 1BJ, United Kingdom

ARTICLE INFO

Keywords:
A ring-stiffened cylindrical shell
Force excitation
Acoustic excitation
Experiment

ABSTRACT

Taken a submerged ring-stiffened cylindrical shell as an experimental model, the experimental studies was investigated to study the effects of force and acoustic excitation on the vibro-acoustic response of the cylindrical shell. A precise transfer matrix method (PTMM) was presented to compare the shell vibration and sound radiation of the submerged stiffened cylindrical shell with the experimental results. The result shows that results from PTMM are in good agreement with the experimental results. It shows that the PTMM is reliable and the result from PTMM is credible. The vibration acceleration response of the water case has less peak numbers and the value is less than that of the air case. The peak value of sound pressure in the force excitation case is relate to structural natural frequency. The peak value of sound pressure in the acoustic excitation case is relate to structural natural frequency and internal cavity natural frequency.

Introduction

Ring-stiffened cylindrical shells are the typical structural forms in aeronautical or naval industry. There is a considerable amount of literature dealing with the vibration and sound radiation of stiffened cylindrical shells and much attention on the dynamic behaviors of cylindrical shell has been received [1–5]. Some theoretical methods have been developed on the dynamic behaviors of shells, such as wave propagation method [6,7], Fourier spectral element method [8,9], transfer matrix method [10] and so on.

Analytical solutions are hard to be derived with the presence of the fluid load and discontinuities of the stiffened shell. Then semi analytical methods and numerical approach are employed to model the addressed problem. Caresta and Kessissoglou [11–13] used the wave propagation method to solve the structure response and acoustic radiation characteristics of underwater ring stiffened cylindrical shell under axial excitation. They paid more attention on the structural and acoustic of a submarine hull considering effect of propeller forces and harmonic excitation. Meyer et al. [14] had a research on the prediction of the vibro-acoustic behavior of submerged shells with non-axisymmetric internal structures. Wang et al. [15–17] developed a precise transfer matrix method for vibro-acoustic analysis of submerged stiffened combined shell and conical shell by solving a set of first order differential equations. Qu et al. [18–20] presented a modified variational method for free and forced vibration analysis of ring-stiffened conical-cylindrical and conical-cylindrical-spherical shells subjected to different boundary conditions, and used the discrete element stiffener theory to consider the ring-stiffening effects.

Numerical method such as finite element method (FEM) and boundary element method (BEM) have the advantages to model vibro-acoustic behavior of arbitrary complex structure, but actually the development of FEM and BEM is limited by many problems. Based on the discrete element meshes and constructing the low order shape functions to solve the fluid-structure interaction problem, its solution accuracy is restricted by frequency band. The number of elements will increase sharply as the frequency increases, which seriously reduces computational efficiency and increases storage space. Ettouney et al. [21] investigated vibrational and acoustical characteristics of a submerged cylindrical shell with two hemispherical end closures and an interior beam. A finite difference method was adopted to model the shell and the beam was tackled using FEM. Marcus [22] performed A finite element analysis on a submerged cylindrical shell with internal frames and point masses attached to the frames. A point force on the shell is shown to excite resonances of the frames. A fully coupled finite element/boundary element (FE/BE) model has been developed to investigate the effect of mass distribution and isolation in a submerged hull [23].

* Corresponding author at: Departments of Naval Architecture, Ocean and Structural Engineering, School of Transportation, Wuhan University of Technology, Wuhan 430063, PR China.
E-mail address: xianzhongwang00@163.com (X. Wang).

https://doi.org/10.1016/j.rinp.2018.09.017
Received 18 July 2018; Received in revised form 16 August 2018; Accepted 7 September 2018
Available online 13 September 2018

Meyer et al. [24] developed the Condensed Transfer Functions (CTF) method to study vibrations and acoustics of cylindrical shells with more complicated interior frames. Chen et al. [25,26] developed a hybrid approach combining WBM and FEM is presented to investigate vibration characteristics of a cylindrical shell coupled with interior structures.

Due to the operation of internal machinery and equipment, radiation noise of cylindrical shells is generated by two kinds of motivation: force excitation and acoustic excitation. To the authors' knowledge, there are some but not many literature concerning vibro-acoustic behavior of stiffened cylindrical shells with force and acoustic excitation. Farshidianfar et al. [27] used two other methods along with was to excite a long circular cylindrical shell, with acoustical excitation and simply supported boundary conditions.

The aim of the present work is to discuss experimental results of a stiffened cylindrical shell with force and acoustic excitation. The authors setup the experiment model and ran the model test to free vibration, forced vibration and acoustic response of the cylindrical shell in fluid. The authors also employ precise transfer matrix method (PTMM) [15] to solve the first order differential equations for modelling vibro-acoustic behavior of the stiffened submerged cylindrical shell. The vibration of the cylindrical shell is obtained by assembling the segment field transfer matrixes of the cylindrical shell and point transfer matrixes of the ring-stiffener. Based on Moore-Penrose pseudoinverse method, the radiated noise of the cylindrical shell can be solved by taking collocation points on the fluid-structure interaction interface. Then the calculated results are compared with the experimental results. Also, the effect of the external excitation on the acoustic response of the cylindrical shell is investigated.

Experimental research

Experimental model

The test model is a single ring-stiffened cylindrical shell, as shown in Fig. 1. Welding was not considered to guarantee the accordance with the theoretical model. The cylindrical shell has the following material properties: Length $L = 0.8$ m, Radius $R_1 = 0.3$ m. Shell thickness $t = 4$ mm. sectional dimensions of the stiffener is 40 mm × 4 mm. The stiffeners spacing $\Delta l = 0.16$ m. The density of the material $\rho = 7850$ kg/m^3, the elastic modulus of the material $E = 203$ GPa and the Poisson's ratio $\nu = 0.3$. 15 mm thick caps are screwed at the ends of the cylinder. This stiffened cylindrical shell is referred to as the axisymmetric case, which is equipped with a fixed exciter and primary sound source. The function of the external hoisting model is achieved by welding the lifting lug at the end cover.

Experimental setup

The cylindrical shell vibration measurement system is mainly composed of anechoic tank, vibration exciter, hammer, power amplifier, signal generator, data acquisition device, force sensor, acceleration sensor and hydrophone. The anechoic tank is 8 m long, 4 m wide and 3 m deep. The cuneiform sound absorption cone is arranged on the six surface of the pool, anechoic tank and test model are shown in Fig. 2.

A 10 mm diameter patch is glued on the inner surface of the cylindrical shell, and screwed to a shaker (DH-40020). The shaker is fixed on the end cap in order to excite the point of coordinate (x, r, θ) = (0.4 m, 0.3 m, 0) in the cylindrical system (with $x = 0$ at the bottom of the cylindrical shell). The measurement excitation is 1 N sinusoidal excitation. There are two components between the patch and the shaker: an impedance head (PCB-208c02) that measures acceleration and force at the excitation point, and a threaded rod that allows assuming a radial excitation in the cylindrical system. A flexible rope is used to connect the shop crane above the anechoic tank, and the heavy load is laid on the top cover of the model to keep balance. There are 8 acceleration sensors (PCB-352c03) to measure the radial vibration acceleration on the outer surface of the cylindrical shell for the four configurations, which include free vibration and forced vibration in air and fluid. Taking account of axisymmetric features, several measuring points along the axial and circumferential direction are arranged to record the vibration responses. The positions of 8 sensors are located at position1 (0.4 m, 0.3 m, 0), position2 (0.48 m, 0.3 m, 0), position3 (0.56 m, 0.3 m, 0), position4 (0.64 m, 0.3 m, 0), position5 (0.72 m, 0.3 m, 0), position6 (0.4 m, 0.3 m, $\pi/4$), position7 (0.4 m, 0.3 m, $\pi/2$), position8 (0.4 m, 0.3 m, π). The layout of measuring points is shown as Fig. 2.

PTMM for stiffened cylindrical shell

Field transfer matrix for the cylindrical shell

A schematic diagram of the stiffened cylindrical shell is shown in Fig. 3. h denotes the thickness of the cylindrical shell, L denotes the length of the cylindrical shell, and R denotes the radius of the cylindrical shell. Based on Flügge shell theory, it can be written as a matrix differential equation [15]

$$\frac{d\boldsymbol{Z}(\xi)}{d\xi} = \mathbf{U}(\xi)\boldsymbol{Z}(\xi) + \boldsymbol{F}(\xi) - \boldsymbol{p}(\xi) \tag{1}$$

where $\boldsymbol{Z}(\xi) = \{u_* \; v_* \; w_* \; \psi_* \; M_{s^*} \; V_{s^*} \; S_{s\theta^*} \; N_{s^*}\}^{\mathrm{T}}$, u_*, v_*, w_*, ψ_*, M_{s^*}, V_{s^*}, $S_{s\theta^*}$ andN_{s^*} are the dimensionless axial, circumferential, radial displacements, angular angle, moment, radial, circumferential and axial forces. $\mathbf{U}(\xi)$ is the field transfer matrix for the state vector of the cylindrical shell. ξ is the dimensionless axial position. The nonzero elements in

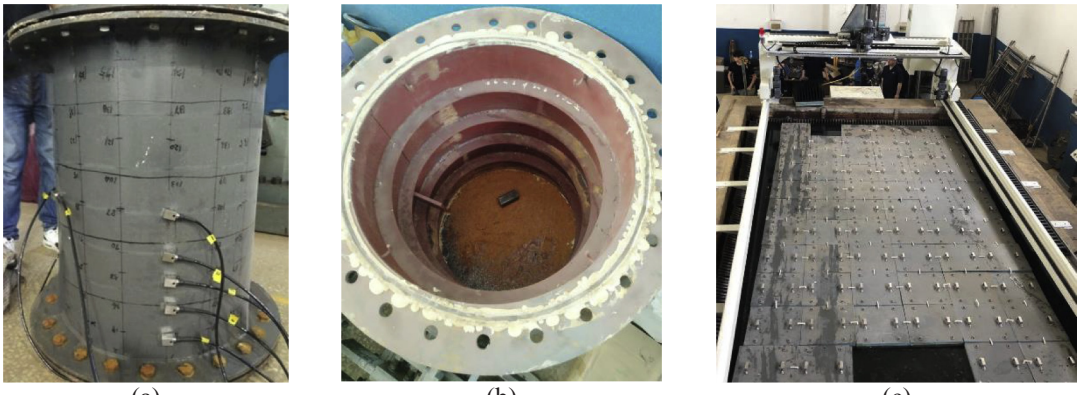

(a) (b) (c)

Fig. 1. Pictures of an axisymmetric stiffened cylindrical shell: (a) hanged on a rope and (b) interior view. (c) anechoic tank with a running gear.

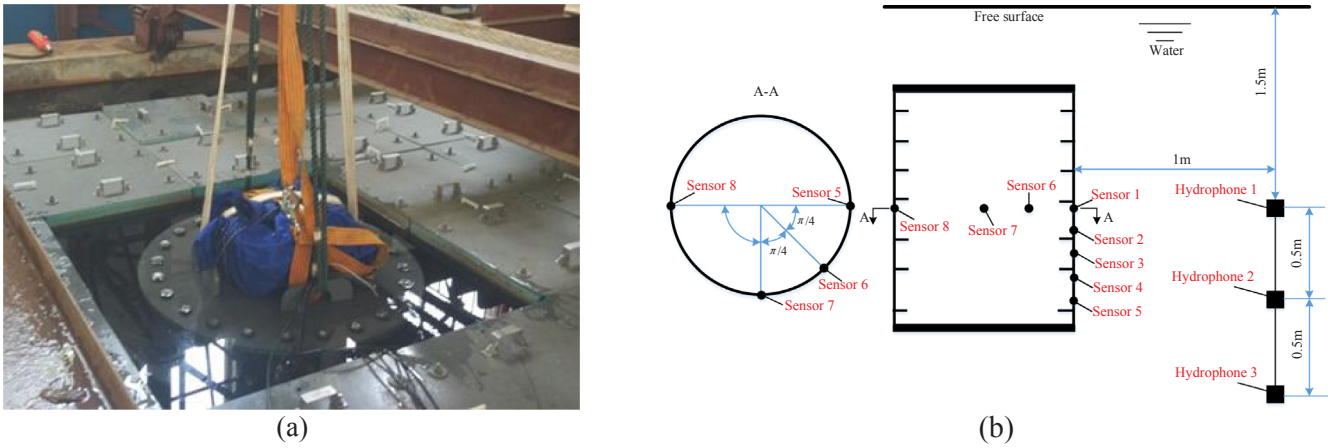

Fig. 2. Experimental setup for the stiffened cylindrical shell submerged in water: (a) The measurement excitation system and (b) The layout of measuring points.

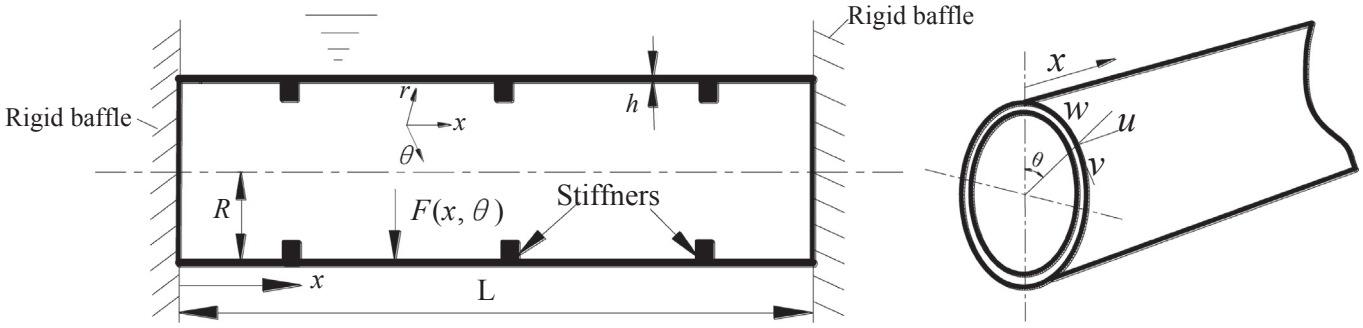

Fig. 3. Scheme for the stiffened cylindrical shell.

Table 1
Comparison of the coupled natural frequencies (unit: Hz).

Mode shape	Present method	FEM	X.M. Zhang's method [28]	Difference
$m = 1, n = 2$	4.94	4.92	4.95	−0.41%
$m = 1, n = 3$	8.91	9.06	8.95	1.66%
$m = 2, n = 3$	10.86	10.71	10.66	−1.40%
$m = 2, n = 2$	11.56	11.24	11.54	−2.85%
$m = 3, n = 3$	14.68	14.7	14.73	0.14%
$m = 1, n = 4$	18.24	18.68	18.26	2.36%
$m = 2, n = 4$	18.68	19.14	18.71	2.40%
$m = 3, n = 4$	20.14	20.37	20.00	1.13%

Table 2
Comparison of natural frequencies of the cylindrical shell in air case (unit: Hz).

Order number	1 (2,1)	2 (3,1)	3 (1,2)	4 (1,3)	5 (1,4)
Experiment	356.6	854.1	1047.3	1222.3	1265.2
PTMM	342.69	833.72	1011.7	1178	1272.5
%Error	4.0	2.4	3.5	3.8	0.6
Order number	6 (2,4)	7 (3,3)	8 (3,4)	9 (3,5)	10 (2,5)
Experiment	1341.7	1399.1	1474.0	1539.4	2061.9
PTMM	1318.8	1326.1	1421.8	1509.5	2064.3
%Error	1.7	5.5	3.7	2.0	0.1

$\mathbf{U}(\xi)$ are given in Ref. [15].

The general solution for the linear inhomogeneous dynamic Eq. (1) could be expressed as

$$\boldsymbol{Z}(\xi) = e^{\boldsymbol{U}\Delta\xi}\boldsymbol{Z}(\xi_0) + \int_{\xi_0}^{\xi} e^{\boldsymbol{U}(\xi-\tau)}\boldsymbol{r}(\tau)d\tau \tag{2}$$

in which $\boldsymbol{r}(\tau) = \boldsymbol{F}(\xi) - \boldsymbol{p}(\xi)$, and $\int_{\xi_0}^{\xi} e^{\boldsymbol{U}(\xi-\tau)}\boldsymbol{r}(\tau)d\tau$ is the state response resulted from inhomogeneous items.

The cylindrical shell can be divided into series of segments, with the

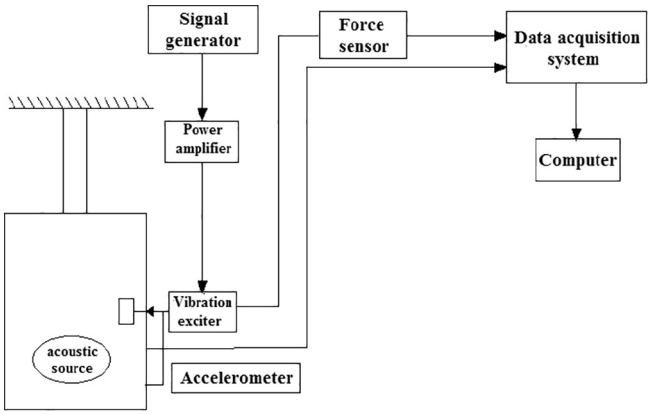

Fig. 4. Schematic diagram of forced vibration test.

node coordinates being ξ_k, $k = 1,2,3,\ldots,N-1$ respectively. Therefore, the adjacent coordinates are ξ_k and ξ_{k+1}, and $\xi_{k+1} = \xi_k + \Delta\xi$. Hence, they have the following relation

$$\boldsymbol{Z}(\xi_{k+1}) = e^{\boldsymbol{U}\Delta\xi}\boldsymbol{Z}(\xi_k) + \int_{\xi_k}^{\xi_{k+1}} e^{\boldsymbol{U}(\xi_{k+1}-\tau)}\boldsymbol{r}(\tau)d\tau = \boldsymbol{\Phi}_0(\Delta\xi)\boldsymbol{Z}(\xi_k) + \int_0^{\Delta\xi} e^{\boldsymbol{U}\tau}\boldsymbol{r}(\xi_{k+1}-\tau)d\tau \tag{3}$$

where $\boldsymbol{\Phi}_0(l) = e^{\boldsymbol{U}\Delta\xi}$ can be solved by using precise integration method [15].

Point transfer matrix for the stiffener

The effects of the stiffener acting on cylindrical shell are mainly manifested in the variation of the state vector. At a position ξ_k, where the stiffener and the cylindrical shell are joined together, both forces

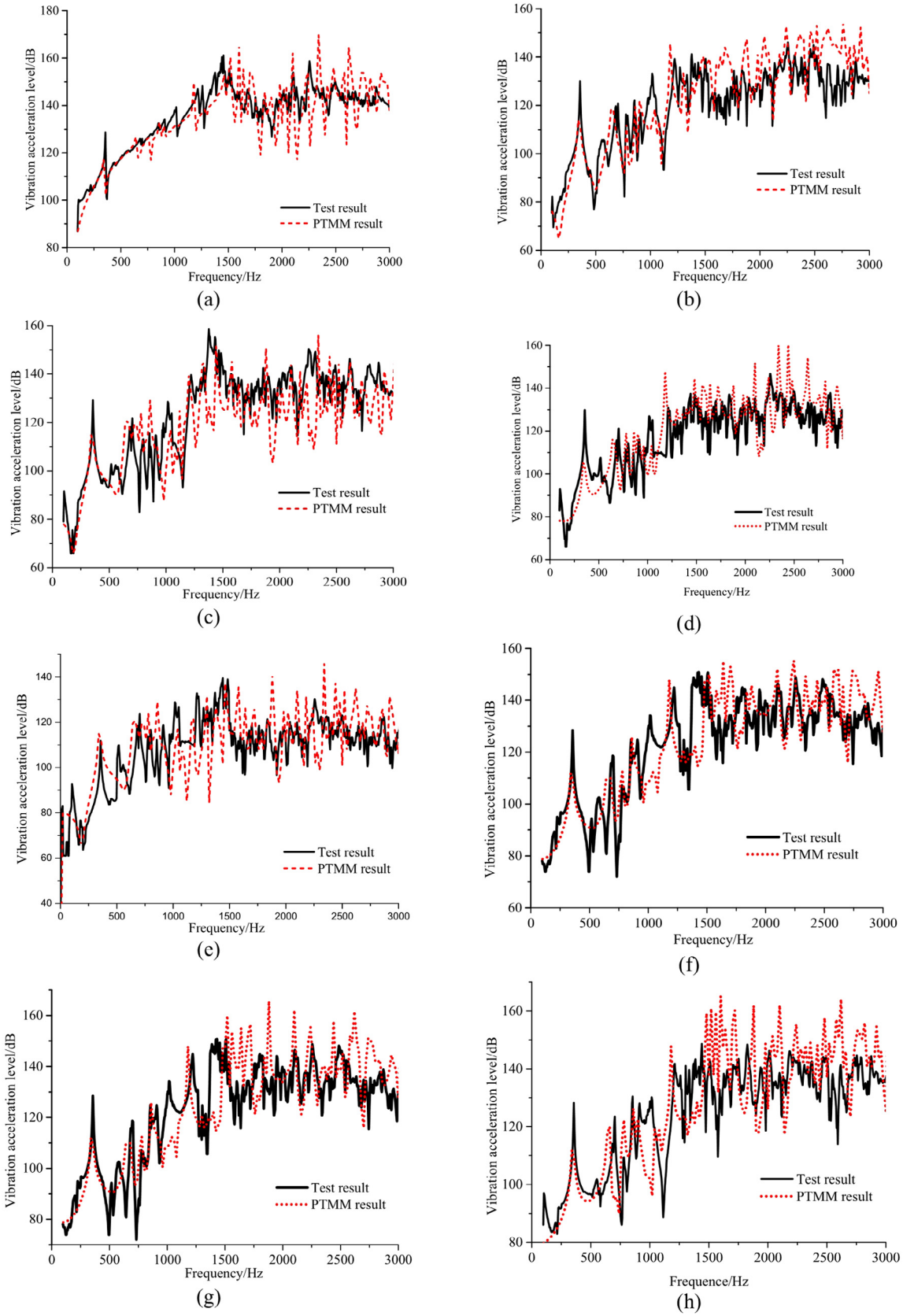

Fig. 5. The forced vibration response of the cylindrical shell in the air: (a) position1, (b) position2, (c) position3, (d) position4, (e) position5, (f) position6, (g) position7, (h) position8.

Table 3
The first tenth natural frequencies of the test model in the air and in the water (unit: Hz).

Order number	1 (2,1)	2 (3,1)	3 (1,2)	4 (1,3)	5 (1,4)
In the Air	356.6	854.1	1047.3	1222.3	1265.2
In the Water	231.4	445.9	644.5	723.2	956.3
Order number	6 (2,4)	7 (3,3)	8 (3,4)	9 (3,5)	10 (2,5)
In the Air	1341.7	1399.1	1474.0	1539.4	2061.9
In the Water	1021.8	1114.1	1263.4	1326.5	1621.3

within and out of plane have been changed between left end ξ_k^L and right end ξ_k^R of the stiffener. The state vectors satisfy

$$\boldsymbol{Z}(\xi_k^R) = \boldsymbol{Tr}_k \boldsymbol{Z}(\xi_k^L) \tag{4}$$

where $\boldsymbol{Z}(\xi_k^L)$ and $\boldsymbol{Z}(\xi_k^R)$ represent state vectors of the left end and the right end, respectively. $\boldsymbol{Tr}_k$ is the point transfer matrix of order 8×8.

Acoustic response formula

The finite stiffened cylindrical shell is terminated by infinite rigid baffles and immersed in an infinite acoustic medium (see Fig. 1). For ideal fluids, the pressure p satisfies the Helmholtz equation

$$\nabla^2 p + k_0^2 p = 0 \tag{5}$$

where $k_0 = \omega/c_0$, $\omega$is the angular frequency and c_0 is the speed of sound. Continuity of mechanical and acoustic velocities results in

$$-\frac{1}{i\omega\rho}\frac{\partial p}{\partial r} = \frac{\partial w}{\partial t}\bigg|_{r=R}, \quad 0 \le x \le L \tag{6}$$

where ρ is the fluid density. Radiated sound pressure p at infinity point also should satisfy Sommerfeld radiation condition. The solution for the sound pressure at the a field point (r, θ, x) in the external sound field could be written as

$$p = \sum_{\alpha=0}^{1}\sum_{n=0}^{\infty}\sum_{m=0}^{\infty} p_{mn} H_n^{(1)}(k_r r)\cos(k_m x)\sin\left(n\theta + \frac{\alpha\pi}{2}\right) \tag{7}$$

where $k_m = \frac{m\pi}{L}$, $m = 0, 1, \ldots N$, $k_r = \sqrt{k_0^2 - k_m^2}$.

External force

Assuming the mechanical force acting on the point (x_0, θ_0) of the shell or the stiffener is concentrated force, it can be expressed as [29,30]

$$f(x, \theta) = f\delta(x - x_0)\delta(\theta - \theta_0)/R \tag{8}$$

After orthogonal transformation of Eq. (41), one obtains

$$f(x, \theta) = \delta(x_0)\sum_{\alpha=0}^{1}\sum_{n=0}^{\infty} f_n \sin\left(n\theta + \frac{\alpha\pi}{2}\right) \tag{9}$$

where

$$f_n = \sum_{\alpha=0}^{1} f_0 \frac{\varepsilon_n}{2\pi R}\sin\left(n\theta_0 + \frac{\alpha\pi}{2}\right), \quad \varepsilon_n = \begin{cases} 1, & n = 0 \\ 2, & n \ne 0 \end{cases}.$$

Vibration response solution

The transfer relation between the state vectors of both ends of the jth segment $\xi_j - \xi_{j+1}$ is analyzed. Assuming there is a rib at ξ_i in the jth segment, the left state vector $\boldsymbol{Z}^L(\xi_i)$ of the cross section can be expressed as

$$\boldsymbol{Z}^L(\xi_i) = \exp[\boldsymbol{U}(\xi_i - \xi_j)]\boldsymbol{Z}(\xi_j) + \int_{\xi_j}^{\xi_i} \exp[\boldsymbol{U}(\xi_i - \tau)]\boldsymbol{r}(\tau)d\tau \tag{10}$$

The state vectors of the cross section where the rib is laid satisfy Eq. (10), that is $\boldsymbol{Z}(\xi_i^R) = \boldsymbol{Tr}_i \boldsymbol{Z}(\xi_i^L)$. $\boldsymbol{Tr}_i$ represents the point transfer matrix of the ith rib. Then one can obtain

$$\boldsymbol{Z}(\xi_{j+1}) = \boldsymbol{Z}_{j+1}\boldsymbol{Z}(\xi_j) + \boldsymbol{P}_{j+1}, \quad j = 1, \ldots, N-1 \tag{11}$$

where $\boldsymbol{T}_{j+1} = \exp[\boldsymbol{U}(\xi_{j+1} - \xi_j)]$, $\boldsymbol{P}_{j+1} = \int_{\xi_j}^{\xi_{j+1}} \exp[\boldsymbol{U}(\xi_{j+1} - \tau)]\boldsymbol{r}(\tau)d\tau$.

The equations of the whole structure can be obtained by assembling Eq. (11), according to the boundary conditions of two ends, finding the line numbers of the determinate state vectors in $\boldsymbol{Z}(\xi_1)$, $\boldsymbol{Z}(\xi_N)$, and deleting the corresponding row in the coefficient matrix, then The equations of the whole structure can be expressed as

$$\begin{bmatrix} -\boldsymbol{T}_2 & \boldsymbol{I}_8 & 0 & 0 & 0 & 0 \\ 0 & -\boldsymbol{T}_3 & \boldsymbol{I}_8 & 0 & 0 & 0 \\ 0 & 0 & -\boldsymbol{T}_4 & \boldsymbol{I}_8 & 0 & 0 \\ 0 & 0 & 0 & \ldots & \boldsymbol{I}_8 & 0 \\ 0 & 0 & 0 & 0 & -\boldsymbol{T}_N & \boldsymbol{I}_8 \end{bmatrix} \begin{Bmatrix} \boldsymbol{Z}(\xi_1) \\ \boldsymbol{Z}(\xi_2) \\ \boldsymbol{Z}(\xi_3) \\ \vdots \\ \boldsymbol{Z}(\xi_N) \end{Bmatrix} = \begin{Bmatrix} \boldsymbol{P}_2 \\ \boldsymbol{P}_3 \\ \boldsymbol{P}_4 \\ \vdots \\ \boldsymbol{P}_N \end{Bmatrix} \tag{12}$$

Expansion of the determinant of the amplitude coefficient in Eq. (12) provides the dispersion equation of the cylindrical shell

$$D(n, \omega) = 0 \tag{13}$$

Sound radiation solution

Using the linear superposition principle, for a given nth circumferential mode, the corresponding radial displacement satisfies the following equation

$$w^n(x) = w_f^n(x) + \sum_{m=0}^{\infty} p_{mn} w_m^n(x) \tag{14}$$

here, $w_f^n(x)$ denotes the radial displacement of shell under concentrated force with a circumferential number order n, and $w_m^n(x)$ denotes the radial displacement of shell under sound pressure excitation with a wave number (m, n).

Any point at the interface should meet Eq. (6). Functions interpolated by orthogonal polynomials in evenly spaced points fail to converge for$N \to \infty$. Interpolation points number N should satisfy two conditions: greater than wave number m and $N \ge 2\pi\lambda^{-1}$. The equation for solving the corresponding sound pressure coefficients can be obtained

$$\sum_{m=0}^{\infty} p_{mn}\left(\frac{\partial H_n^{(1)}(k_r R)}{\partial r}\cos(k_m x_j) - \rho_0\omega^2 w_m^n(x_j)\right) = w_f^n(x_j), \quad j = 1, 2, 3\ldots M \tag{15}$$

p_{mn} can be solved using Moore-Penrose pseudoinverse method. Substituting p_{mn} into Eq. (7), one can obtain the sound pressure in fluid field.

Validation studies

Free vibration

The focus of this section is to validate the accuracy of the present method for calculating coupled natural frequency of cylindrical shell submerged in a fluid medium. The geometric and physical parameters for the selected cylindrical shell [28] are: length $L = 20$ m, radius $R = 1.0$ m, thickness $h = 10$ mm, Young's modulus of elasticity $E = 2.1 \times 10^{11}$ Pa, Poisson's ratio $\mu = 0.3$, and density $\rho = 7850$ kg/m^3. For a clamped cylindrical shell, the natural frequencies for each order can be obtained, which are compared with the results by using FEM as illustrated in Table 3. The difference is between FEM and present method. From Table 1, we can see that, for a cylindrical shell model with clamped condition at both ends, the natural frequencies yielded by adopting precise transfer matrix method which is based on Flügge shell theory are in good agreement with FEM results and X.M.

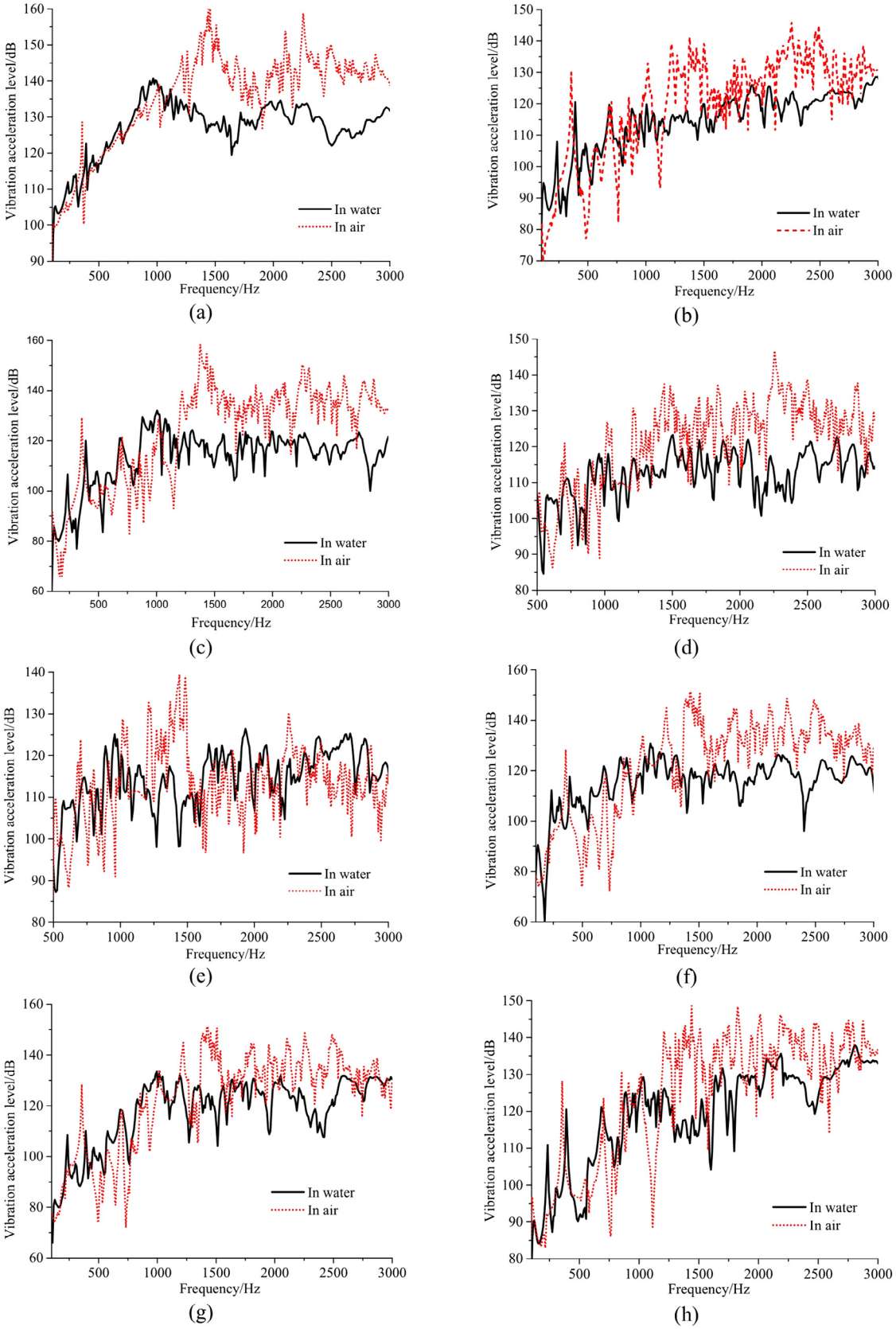

Fig. 6. Results contrast of the forced vibration of the cylindrical shell in the air and water cases: (a) position1, (b) position2, (c) position3, (d) position4, (e) position5, (f) position6, (g) position7, (h) position8.

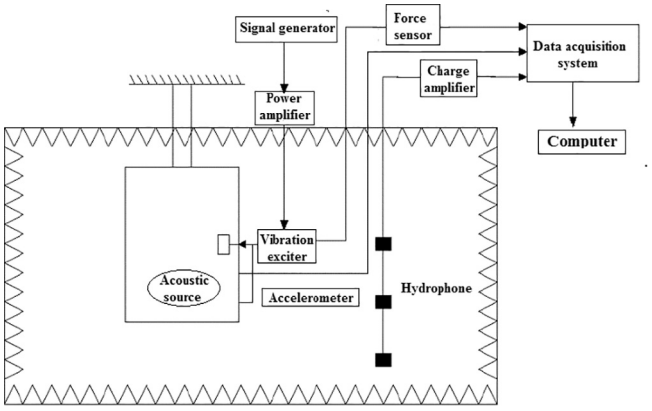

Fig. 7. Schematic diagram of underwater acoustic radiation test in water.

Zhang's method. The relative difference is less than 3%, which proves that precise transfer matrix method is correct.

The acceleration sensors stuck to the measuring points, are connected with the data acquisition system. A force hammer is employed to knock structure model, a free vibration test of a cylindrical shell hoisted by a flexible rope is carried out, the natural frequency and structural mode in air can be obtained by the vibration response analysis processing module in the system. To ensure the accuracy of vibration response calculation, the experimental results are compared with the natural frequencies of cylindrical shell model established by PTMM. The modal test was carried out using the impact hammer PCB 086C03 and the accelerometers PCB 353B15. The test results of natural frequencies of the first 10 orders of the model are given in Table 2.

Table 2 summarizes the theoretical and experimental natural frequencies. Table 2 shows that the theoretical natural frequencies in vacuo are in good agreement with ones in air. And the theoretical natural frequencies in vacuo are slightly lower than the experimental natural frequencies in water except for the (1, 4) mode. It is due to the fact that the baffled shell theory for the fluid-structure interaction constrains the fluid motion because of artificial rigid cylinders attached to both ends of the cylindrical shell, thus increases the kinetic energy of the fluid, and in turn increases the virtual fluid mass.

Forced vibration

The forced vibration test with the vibrator and the non-directional dodecahedron sound source excitation is carried out in air and water. In the test process, a single frequency sinusoidal signal is produced by the signal generator as the input signal, and the power amplifier is driven to amplify the signal. In the case of acoustic and force excitation with the linear sweep frequency (100 Hz–2000 Hz), the schematic of forced vibration test in air is shown as Fig. 4. The measured data of the acceleration sensors are converted into a vibration acceleration level by $L_a = 20\lg(a/a_0)$, where a is the experimental test data and a_0 is the base acceleration $1e-6\ m/s^{-2}$.

In the air case, the acceleration data of the measured points is processed to get the vibration acceleration level in the frequency range. PTMM is employed to calculate the vibration response of the experimental model. The boundary condition of the both end is clamped. In this experiment, only the vibration response with the force excitation is compared with the result from PTMM, as shown in Fig. 5. It can be observed that in the 100–1000 Hz band, the result from PTMM in vacuo are in good agreement with test result in air. The vibration response is slightly different at the resonance peak value, and the PTMM's peak value is slightly lower than the experimental value in Fig. 5. In particular at middle frequency between 1000 and 1500 Hz, there are some resonance peaks lost for PTMM, compared with the test result. Even there are some corresponding frequencies difference in peaks between

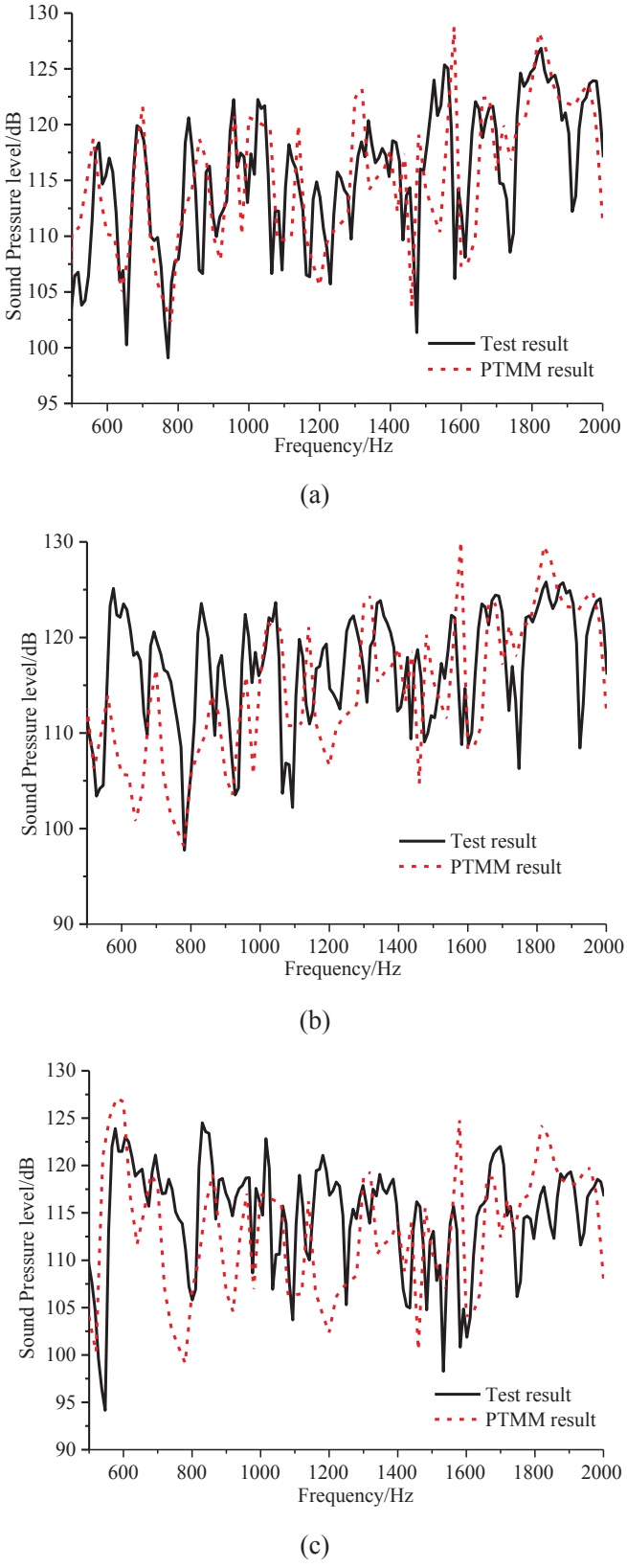

Fig. 8. Comparison of the sound pressure of the cylindrical shell with force excitation between test and PTMM: (a) hydrophone 1, (b) hydrophone 2, (c) hydrophone 3.

two results. In the frequency up to 3000 Hz, the peak numbers of test are much more than that of PTMM, which have acute fluctuation appeared in peak position and phase advance. In authors' opinion, it is

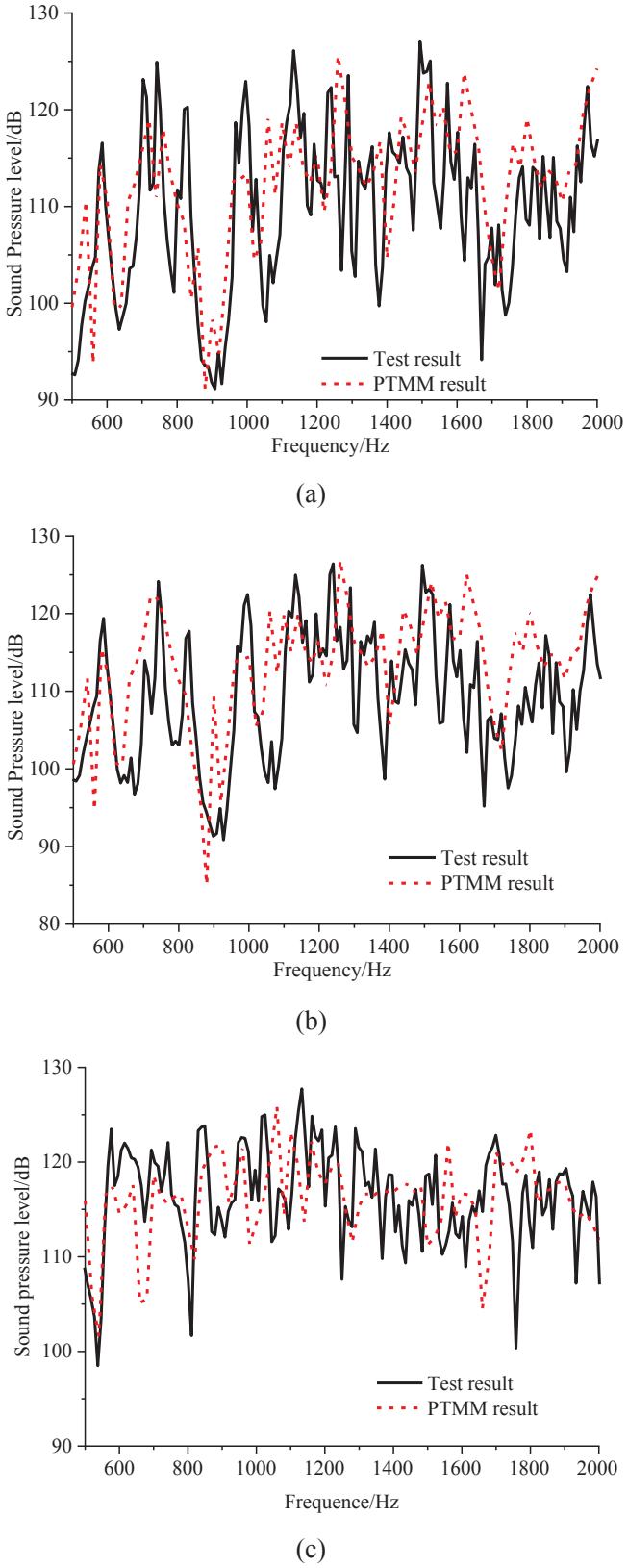

Fig. 9. Comparison of the sound pressure of the cylindrical shell with acoustic excitation between test and PTMM: (a) hydrophone 1, (b) hydrophone 2, (c) hydrophone 3.

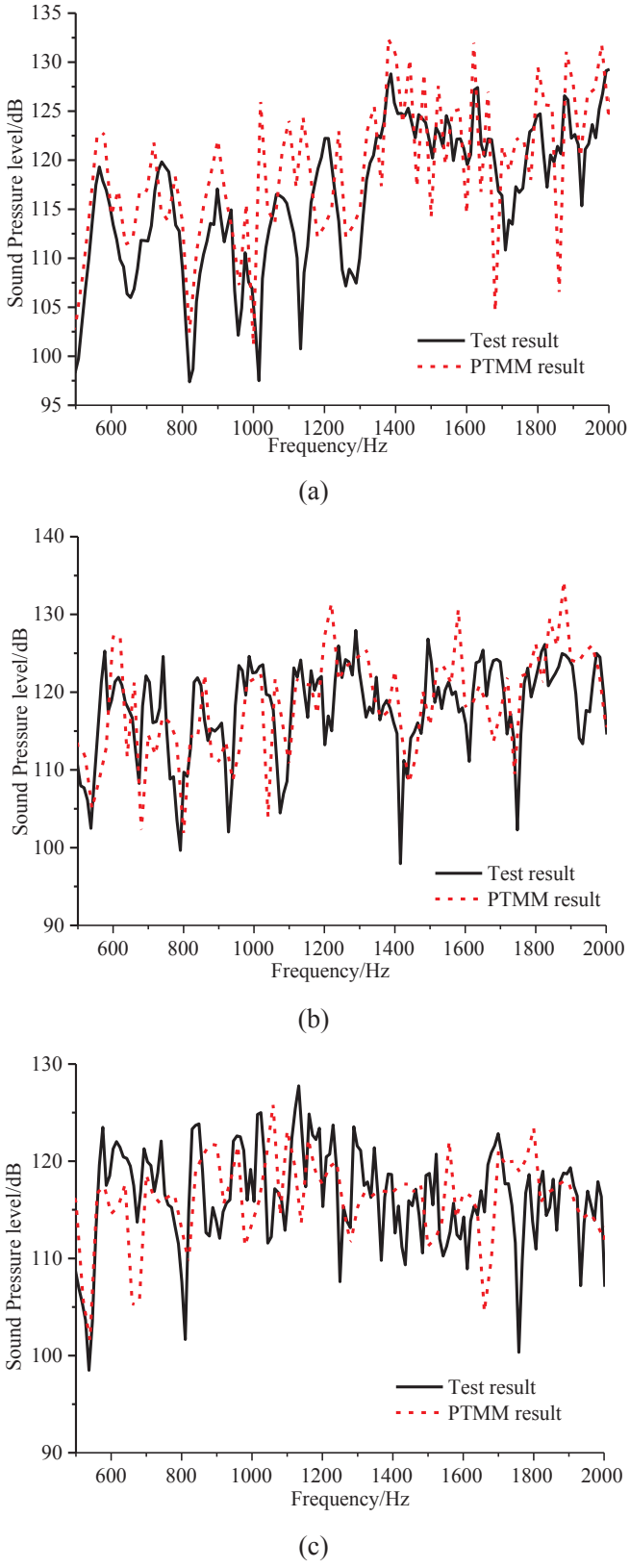

Fig. 10. Comparison of the sound pressure of the cylindrical shell with force and acoustic excitation between test and PTMM: (a) hydrophone 1, (b) hydrophone 2, (c) hydrophone 3.

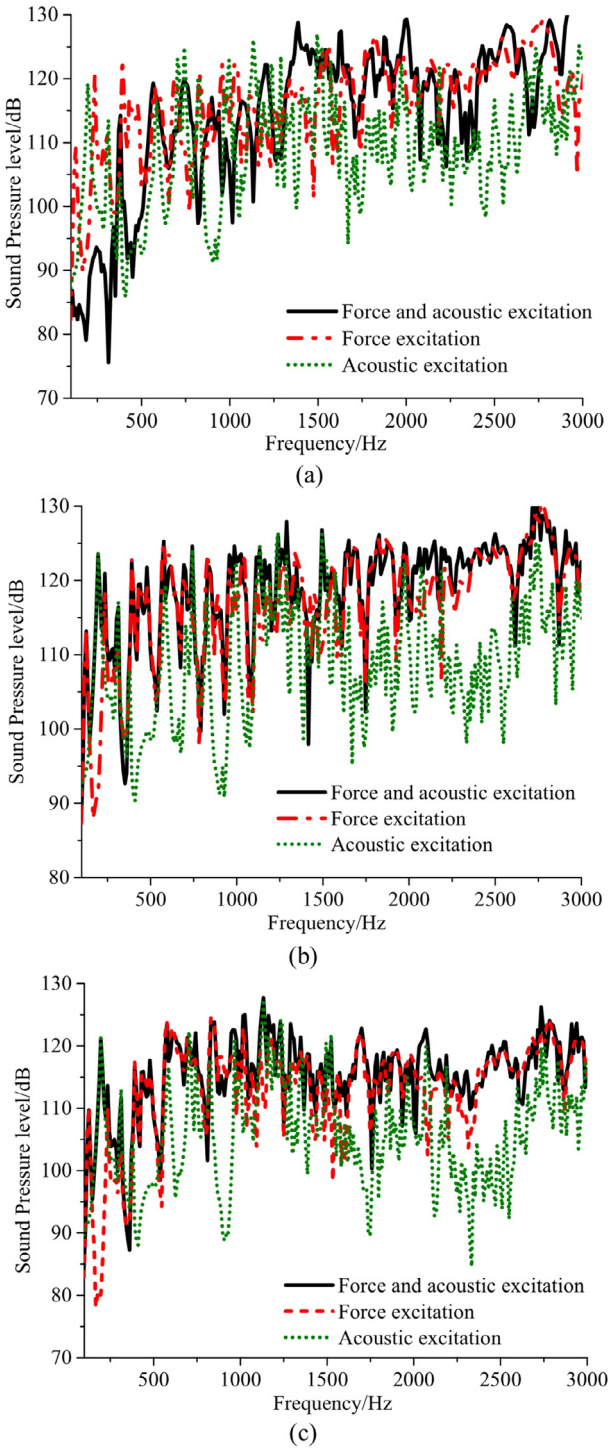

Fig. 11. Comparison of sound pressure level of the measurement point under different excitations: (a) hydrophone 1, (b) hydrophone 2, (3) hydrophone 3.

mainly due to the local vibration of the structure caused by the end cap and seal flange. Also, in actual working conditions, the actual boundary conditions cannot be completely similar to the PTMM's clamped boundary, and the PTMM is much more optimized. In general, the results from PTMM are in good agreement with the vibration trend of the experimental result. It shows that the PTMM is reliable and the result from PTMM is credible.

Table 3 gives the first ten natural frequencies of the model in the air and in the water. The natural frequency of the cylindrical shell in the water is lower than that in the air condition. It also shows that the added mass resulted from the fluid load on the mode of the shell cannot be ignored. The forced vibration response test of the cylindrical shell submerged in water is carried out in frequency range 100–3000 Hz, as shown in Fig. 6. The comparative analysis between the natural frequency result in Table 3 and the peak frequencies of acceleration response of measurement points in Fig. 6 show that regardless of the air case and water case, the first ten natural frequencies are consistent with the peak frequencies under force excitation. The forced vibration of the shell in the water has less peak numbers than the situation in air, but it is basically consistent with the air case in frequency range (100–1000 Hz). There is an obvious difference between the both cases in the middle and high-frequency range (1000 Hz–3000 Hz). The vibration acceleration response of the water is less than the value in the air.

Acoustic radiation

The two end caps and the cylindrical shell are sealed with water sealant, and submerged into the anechoic tank, as shown in Fig. 7. The input signal is generated by the signal generator, which drives the shaker and the non-directional dodecahedron sound source to work. The radiation medium is water, the water density is 1000 kg/m^3, the velocity of sound in water is 1500 m/s. Then the noise radiated into the water is resulted from the surface vibration of the cylindrical shell. The excitation is a chirp (swept-frequency sine), and the output is the transfer function with regard to the excitation force. There are 3 hydrophone (BK-8104) is placed 1.0 m far from the cylindrical shell's surface as seen in Fig. 2b, which were setup in the anechoic tank to measure the sound pressure. In the case of sound and force excitation with the linear sweep frequency (100 Hz–3 kHz), a schematic diagram of the vibration and underwater acoustic radiation test is shown in Fig. 7. The data measured by the hydrophone is converted into a sound pressure level by $L_p = 20\lg(p/p_0)$, where p is the experimental test data and p_0 is the base acceleration 1 μPa.

Comparison between the experimental and PTMM's results of the sound pressure of measuring points in the force excitation case is shown in Fig. 8. Comparison between the experimental and PTMM's results of the sound pressure of measuring points in the acoustic excitation case is shown in Fig. 9. Comparison between the experimental and PTMM's results of the sound pressure of measuring points in the force and acoustic excitation case is shown in Fig. 10. It can be observed that although the sound pressure is slightly different at the resonance peak value in the 500–2000 Hz band, the sound pressure result from PTMM basically is in accord with test result in water. When the internal medium of the experimental model is full of air, the coupling between structural mode and acoustic cavity mode has little effect on the vibro-acoustic response of the cylindrical shell under force excitation. When shells are excited by force excitation, the sound radiation calculated by PTMM is related to structural vibration mode. This suggest that the coupling can be neglected. A small investigation is carried out and the result totally corresponds with the previous conclusion in compare results of the vibration. The result of PTMM is lack of some resonance peaks relative to the test result at frequency range 1000–1500 Hz. It is also a good proof to verify the conclusion.

Comparison of sound pressure level of the measurement point under different excitations is shown in Fig. 11. From the comparison of sound pressure level under force excitation with that under acoustic excitation, it can be observed that there is significant difference in peak frequencies and peak numbers. The main difference between both cases is that some peak values only exist in the case of force excitation in low frequency range and some peak values only exist in the case of acoustic excitation in middle frequency range. This suggest that the peak value of sound pressure in the force excitation case is relate to structural natural frequency. The peak value of sound pressure in the acoustic excitation case is relate to structural natural frequency and internal cavity natural frequency. In general, the variation trend of sound

pressure level in force excitation is basically consistent with that of sound pressure level in force and acoustic excitation. In frequency range 100–1500 Hz, sound pressure level between force excitation and acoustic excitation keep almost same orders of magnitude, with small difference in peak values. However sound pressure level of acoustic excitation is less than that of force excitation.

Conclusions

In this paper, the experimental test on the vibration and sound radiation of a ring-stiffened cylindrical shell under force excitation and acoustic excitation is studied. The test of vibration and acoustic responses under different excitations are carried out and the experimental data are analyzed. Precise transfer matrix method (PTMM) is used to calculate the forced vibration of the cylindrical shell in air and water and compared with the experimental data. The main conclusions in this paper are as follows:

(1) By comparing the calculated values with the experimental values, it is shown that PTMM is feasible for solving the vibration and acoustic response of the cylindrical shell at low and middle frequencies.
(2) The vibration responses of the cylindrical shell in air and water are obvious different. The forced vibration of the shell in the water has less peak numbers than that of air case, but it is basically consistent with the air case in low frequency range. The vibration acceleration response of the water is less than the value of the air case in middle and high frequency range.
(3) The peak value of sound pressure in the force excitation case is relate to structural natural frequency. The peak value of sound pressure in the acoustic excitation case is relate to structural natural frequency and internal cavity natural frequency.

Acknowledgements

The authors would like to thank the anonymous reviewers for their very valuable comments. This paper was financially supported by the National Natural Science Foundation of China (No. 51779201, 51609190) and Nature Science Foundation of Hubei Province (2018CFB607).

Appendix A. Supplementary data

Supplementary data to this article can be found online at https://doi.org/10.1016/j.rinp.2018.09.017.

References

[1] Leissa AW. Vibration of shells. New York: American Institute of Physics; 1993.
[2] Mukhopadhyay M, Sinha G. Literature review: a review of dynamic behavior of stiffened shells. Shock Vib Dig 1992;24:3–13.
[3] Ruotolo R. A comparison of some thin shell theories used for the dynamic analysis of stiffened cylinders. J Sound Vib 2001;243:847–60.
[4] Ma X, Jin G, Shi S. An analytical method for vibration analysis of cylindrical shells coupled with annular plate under general elastic boundary and coupling conditions. J Vib Control 2015;2:691–3.
[5] Zhang C, Jin G, Ma X. Vibration analysis of circular cylindrical double-shell structures under general coupling and end boundary conditions. Appl Acoust 2016;110:176–93.
[6] Li X. Study on free vibration analysis of circular cylindrical shells using wave propagation. Ship Sci Technol 2009;311:667–82.
[7] Gan L, Li X, Zhang Z. Free vibration analysis of ring-stiffened cylindrical shells using wave propagation approach. J Sound Vib 2009;326:633–46.
[8] Jin G, Ma X, Liu Z. Dynamic analysis of general rotationally symmetric, built-up structures using a modified Fourier spectral element approach. J Vib Acoust 2017;139:021012–21013.
[9] Su Z, Jin G. Vibration analysis of coupled conical-cylindrical-spherical shells using a Fourier spectral element method. J Acoust Soc Am 2016;140:3925–40.
[10] Irie T, Yamada G, Muramoto Y. Free vibration of joined conical-cylindrical shells. J Sound Vib 1984;95:31–9.
[11] Caresta M, Kessissoglou NJ. Structural and acoustic responses of a fluid-loaded cylindrical hull with structural discontinuities. Appl Acoust 2009;70:954–63.
[12] Caresta M, Kessissoglou NJ. Purely axial vibration of thin cylindrical shells with shear-diaphragm boundary conditions. Appl Acoust 2009;70:1081–6.
[13] Caresta M, Kessissoglou NJ. Acoustic signature of a submarine hull under harmonic excitation. Appl Acoust 2010;71:17–31.
[14] Meyer V, Maxit L, Guyader JL, Leissing L. Prediction of the vibroacoustic behavior of a submerged shell with non-axisymmetric internal substructures by a condensed transfer function method. J Sound Vib 2016;360:260–76.
[15] Wang X, Guo W. Dynamic modeling and vibration characteristics analysis of submerged stiffened combined shells. Ocean Eng 2016;127:226–35.
[16] Wang X, Jiang C, Xu R. Structural and acoustic response of a finite stiffened submarine hull. China Ocean Eng 2016;30:898–915.
[17] Wang X, Wu W, Yao X. Structural and acoustic response of a finite stiffened conical shell. Acta Mech Solida Sin 2015;28:200–9.
[18] Qu Y, Chen Y, Long X. Free and forced vibration analysis of uniform and stepped circular cylindrical shells using a domain decomposition method. Appl Acoust 2013;74:425–39.
[19] Qu Y, Hua H, Meng G. A domain decomposition approach for vibration analysis of isotropic and composite cylindrical shells with arbitrary boundaries. Compos Struct 2013;95:307–21.
[20] Qu Y, Wu S, Chen Y. Vibration analysis of ring-stiffened conical-cylindrical-spherical shells based on a modified variational approach. Int J Mech Sci 2013;69:72–84.
[21] Ettouney MM, Daddazio RP, Abboud NN. The interaction of a submerged axisymmetric shell and three-dimensional internal systems. Int J Numer Meth Eng 1994;37:2951–70.
[22] Marcus MH, Houston BH. The effect of internal point masses on the radiation of a ribbed cylindrical shell. J Acoust Soc Am 2002;112:961–5.
[23] Peters H, Kinns R, Kessissoglou NJ. Effects of internal mass distribution and its isolation on the acoustic characteristics of a submerged hull. J Sound Vib 2014;333:1684–97.
[24] Meyer V, Maxit L, Renou Y. Experimental investigation of the influence of internal frames on the vibro-acoustic behavior of a stiffened cylindrical shell using wavenumber analysis. Mech Syst Signal Pr 2017;93:104–17.
[25] Xie K, Chen M, Zhang L. Free and forced vibration analysis of non-uniformly supported cylindrical shells through wave based method. Int J Mech Sci 2017;128:512–26.
[26] Chen M, Zhang L, Xie K. Vibration analysis of a cylindrical shell coupled with interior structures using a hybrid analytical-numerical approach. Ocean Eng 2018;154:81–93.
[27] Farshidianfar A, Farshidianfar MH, Crocker MJ, et al. Vibration analysis of long cylindrical shells using acoustical excitation. J Sound Vib 2011;330:3381–99.
[28] Zhang XM. Frequency analysis of submerged cylindrical shells with the wave propagation approach. Int J Mech Sci 2002;44:1259–73.
[29] Peng YX, Zhang AM, Li SF, et al. A beam formulation based on RKPM for the dynamic analysis of stiffened shell structures. Comput Mech 2018;1:1–14.
[30] Ming FR, Zhang AM, Yao XL. Static and dynamic analysis of elastic shell structures with smoothed particle method. Acta Phys Sin-Ch Ed 2013;62:110203–1148.